

1 Title:

2 **Combining statistical and mechanistic models to identify the drivers of mortality**
3 **within a rear-edge beech population**

4
5 **Authors:**

6 Cathleen Petit-Cailleux¹, Hendrik Davi¹, François Lefèvre¹, Joseph Garrigue², Jean-André Magdalou²,
7 Christophe Hurson^{2,3}, Elodie Magnanou^{2,4}, and Sylvie Oddou-Muratorio¹.

8
9 Adresses

10 ¹INRA, UR 629 Ecologie des Forêts Méditerranéennes, URFM, Avignon, France

11 ²Réserve Naturelle Nationale de la Forêt de la Massane, France

12 ³Fédération des Réserves Naturelles Catalanes, Prades, France

13 ⁴Sorbonne Université, CNRS, Biologie Intégrative des Organismes Marins, BIOM, F-66650 Banyuls-sur-
14 Mer, France

15
16 **Keywords:** *Fagus sylvatica* L., logistic regression, process-based model, dynamic vegetation model,
17 CASTANEA, longitudinal analysis, defoliation.

18

19

20

21

22

23

24

25

26

27

28

29

30

31 **Abstract**

32 Since several studies have been reporting an increase in the decline of forests, a major issue in ecology
33 is to better understand and predict tree mortality. The interactions between the different factors and
34 the physiological processes giving rise to tree mortality, as well as the individual between-tree
35 variability to mortality risk, still need to be identified and assessed.

36 This study is based on a survey of 4323 European beeches (*Fagus sylvatica* L.) since 2002 in a rear-
37 edge population within a natural reserve. We combined two types of approaches: (1) statistical
38 models were used to quantify the effects of competition, tree growth, size and decline on mortality
39 and (2) an ecophysiological process-based model (PBM) was used to separate out the different
40 mechanisms giving rise to temporal and inter-individual variations in mortality by simulating carbon
41 reserves, hydraulic conductance and late frosts in response to climate.

42 The mortality rate at population level was associated to the combination of conductance loss, carbon
43 reserve depletion and occurrence of late frosts simulated with the PBM. In the statistical models, the
44 individual probability of mortality decreased with increasing mean growth, and increased with
45 increasing crown defoliation, earliness of budburst, fungi presence and increasing competition. The
46 interaction between tree size and defoliation was significant, indicating a stronger increase in
47 mortality associated to defoliation in smaller than larger trees. Finally, the PBM predicted a higher
48 conductance loss together with a higher level of carbon reserves for trees with earlier budburst, while
49 the ability to defoliate the crown was found to limit the impact of hydraulic stress at the expense of
50 the accumulation of carbon reserves.

51 We discuss the convergences and divergences obtained between statistical and process-based
52 approaches and we highlight the importance of combining them to identify the different processes
53 underlying mortality, and the factors modulating individual vulnerability to mortality.

54

55

56 Introduction

57 Global changes have been repeatedly reported to be the cause of forest decline and tree
58 mortality, both in terms of background, non-catastrophic mortality (Van Mantgem et al. 2009, Lorenz
59 and Becher 2012) and of massive, catastrophic mortality due to extreme, ‘pulse’ events (Allen et al.
60 2010; Lorenz and Becher 2012; Mueller et al. 2005). To predict how such a new regime of trees
61 mortality will impact upon forest structure, composition and ecosystem services (Anderegg et al.
62 2015a; Choat et al. 2018), we need to better understand the respective roles of the various drivers
63 and mechanisms underlying tree mortality.

64 Studying mortality poses several well-recognized challenges, in particular because it is triggered
65 by several factors and involves several underlying and interacting physiological processes. The factors
66 triggering mortality include extreme, pulse climatic events (i.e. repeated drought, storms, floods,
67 heavy snow, late frosts, wildfires) or sudden changes in biotic interactions (i.e. emerging pests,
68 invasive species), but also long-term climatic or biotic perturbations (i.e. recurrent water deficits,
69 changes in competition at the community level) (Maraun et al. 2003; McDowell et al. 2011).
70 Moreover, these factors can have interactive effects. For instance, drought may increase trees’
71 vulnerability to pests (Durand-Gillmann et al. 2014; Anderegg et al. 2015b) or predispose them to
72 wildfires (Brando et al. 2014). Finally, a single factor triggering mortality may involve several
73 underlying physiological processes, with several thresholds leading to mortality and potential
74 feedback between them (McDowell et al. 2011). This is exemplified by drought, which is usually
75 considered to trigger mortality through the combination of hydraulic failure and carbon starvation
76 (Adams et al. 2017; Anderegg et al. 2012; McDowell et al. 2011). Hydraulic failure is the loss of
77 conductance resulting from major **xylem embolism**, i.e. the formation of water vapour or air bubbles
78 within xylem due to high water tension from soil to canopy (Tyree and Sperry 1989). To avoid
79 hydraulic failure, trees can close their stomata before reaching the **xylem** species-specific embolism
80 point (Cowan and Farquhar 1977). However, stomata closure mechanically reduces photosynthetic
81 activity, forcing the tree to ensure basal metabolism by using carbon reserves, **which can eventually**
82 **become depleted, particularly** during a long period of drought, leading to mortality through carbon
83 starvation. Many experimental studies on drought suggest that hydraulic failure is the most frequent
84 cause of tree mortality, and at least, is often the initial step to trigger a number of interacting
85 processes leading to mortality (Choat et al. 2018). Nevertheless, the relationship between carbon and
86 water fluxes, and the role of biotic factors during and after drought, remains to be clarified (Adams
87 et al. 2017; Feng et al. 2018; McDowell et al. 2011; Meir, Mencuccini, and Dewar 2015; O’Brien et al.
88 2014).

89 Another challenge when studying mortality is that the physiological processes governing tree
90 vulnerability may vary in space and time. For instance, vulnerability may vary among individual trees
91 within a population according to (i) the local spatial heterogeneity of resources availability, especially
92 soil water (Nourtier et al. 2014); (ii) the heterogeneity in an individual tree's life history, and in
93 particular the effects of past stresses on tree morphology and anatomy (Vanoni et al. 2016); (iii) the
94 inter-individual variation of physiological responses to stresses, which depends on ontogenic, plastic,
95 and genetic effects controlling the expression of traits (Anderegg 2015a; Vitasse et al. 2009).
96 Vulnerability may also vary through time for a given individual/population, not only because of
97 temporal climatic variation but also through individual variations in phenological processes. This is
98 well illustrated by the risk of late frost damage, which is closely related to the coincidence between
99 temporal patterns of budburst phenology, and the climatic sequence of low temperatures. Although
100 relatively large safety margins were found regarding the risk of late frost damage during budburst
101 across many European temperate tree and shrub species (Bigler and Bugmann 2018), these safety
102 margins may reduce with climate change, due to budburst in trees occurring earlier (Augspurger
103 2009). When young leaves have been damaged, some species can reflush, i.e. produce another cohort
104 of leaves (Augspurger 2009; Menzel, Helm, and Zang 2015), but the time required to reflush reduces
105 the length of the growing season (Lenz et al. 2013), and may lead to mortality if trees do not have
106 enough reserves to do this.

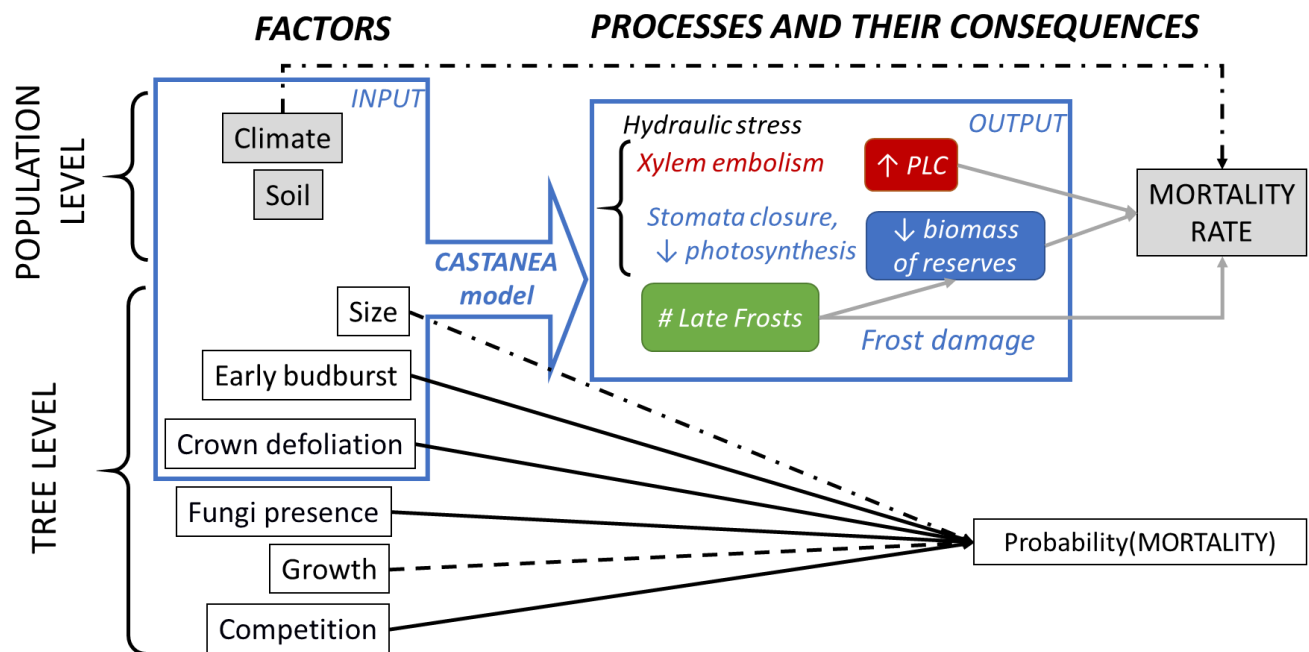
107 Available approaches to investigate the multiple drivers and processes underlying tree mortality
108 can be classified into two broad categories: statistical, phenomenological approaches vs process-
109 based, mechanistic approaches. Statistical approaches use forest inventory data to test how
110 endogenous factors (e.g. related to tree/stand size and growth rate) and exogenous factors (biotic
111 and abiotic environment, including management) [affect stand- or individual- mortality](#). By comparing
112 species or populations over areas with large climatic variations, such studies have demonstrated the
113 overall effect of drought severity on mortality, although usually explaining only a limited proportion
114 of the [variance found in causes of mortality](#) (Allen et al. 2010; Greenwood et al. 2017). Moreover,
115 [probabilities of mortality](#) have been predicted with a higher accuracy when individual covariates for
116 tree growth, size and/or competition were included in the statistical models, highlighting the
117 importance of inter-individual variability in the threshold for mortality (Hülsmann, Bugmann, and
118 Brang 2017; Monserud 1976). Recent statistical studies have attempted to include functional traits
119 involved in the response to stress as additional covariates to improve the accuracy of [mortality](#)
120 [prediction](#). For instance, Carnicer et al. (2011) showed that defoliation trends are consistent with
121 mortality trends in southern European forests. Benito-Garzón et al. (2018) found that mortality

122 increased in populations with negative hydraulic safety margins for 15 species out of the 25 studied.
123 Overall, the main advantage of statistical approaches is their ability to account for a potentially high
124 number of factors and processes triggering mortality and for individual variability in the threshold for
125 mortality. However, these statistical models barely deal with the usually low temporal resolution of
126 mortality data, missing information on the cause of tree death, and non-randomization inherent in
127 natural population designs. In addition, the accuracy of statistical predictions dramatically decreases
128 outside the studied area (Hülsmann, Bugmann, and Brang 2017).

129 On the other hand, biophysical and ecophysiological process-based models (PBMs), initially
130 developed to simulate carbon and water fluxes in forest ecosystems, are also useful to investigate
131 the environmental drivers and physiological processes triggering tree mortality. For example, using
132 the PBM CASTANEA, Davi & Cailleret (2017) showed that mortality of silver fir in southern France
133 resulted from the combination of drought-related carbon depletion and pest attacks. Using six
134 different PBMs, McDowell et al. (2013) found that mortality depended more on the duration of
135 hydraulic stress than on a specific physiological threshold. A main advantage of PBMs is their ability
136 to understand the physiological drivers of mortality and to predict mortality under new combinations
137 of forcing variables in a changing environment. However, they need a large number of parameters to
138 be calibrated, which makes it difficult to have a precise projection in other populations where the
139 model has not been precisely calibrated and validated. Moreover, biophysical and ecophysiological
140 PBMs generally do not take into account individual tree characteristics (i.e. related to ontogenic,
141 plastic and/or genetic variation). Hence, statistical and process-based approaches appear as
142 complementary, and many authors have called for studies comparing or combining them (Hawkes
143 2000; O'Brien et al. 2017; Seidl et al. 2011).

144 An important tree of pan-European forests, the European beech (*Fagus sylvatica* L.) combines
145 a widespread distribution (from northern Spain to southern Sweden and from England to Greece) and
146 a high sensitivity predicted to climate change (Cheaib et al. 2012; Kramer et al. 2010). In particular,
147 bioclimatic niche models predict a future reduction of this species at the rear edge of its range over
148 the next few decades (particularly in the southern part of its distribution), in response to reduced
149 rainfall (Cheaib et al. 2012; Kramer et al. 2010). This prediction is consistent with this species' well-
150 known sensitivity to summer droughts. For example, more frequent extreme droughts have been
151 associated with beech with weaker growth (Dittmar, Zech, and Elling 2003; Jump, Hunt, and Penuelas
152 2006; Knutzen et al. 2017), altered physiological performances (Bréda et al. 2006) and increased
153 defoliation (Penuelas and Boada 2003). However, the low mortality rate observed so far in beech has
154 led some authors to propose that this species presents a higher heat stress tolerance and metabolic

155 plasticity when compared to other tree species (García-Plazaola et al. 2008). This apparent paradox
 156 between a low mortality and a high sensitivity to climate makes beech an interesting model species
 157 to study.



158
 159 **Figure 1: Combining statistical and process-based models to study variables and processes involved**
 160 **in tree mortality at population and tree-level.** The right text in square boxes indicates the measured
 161 factors and response variables considered in statistical models (white background = individual level;
 162 grey background = population level), while the italic text indicates the focal processes (no boxes) and
 163 stress-related output variables (boxes with rounded corners) simulated with the PBM CASTANEA. The
 164 blue box on the left delineates the input variables of CASTANEA. At the top, grey arrows indicate the
 165 relationships considered to link stress-related output variables simulated by CASTANEA with
 166 observed mortality rate at population level, while the thin black arrows indicate the relationships
 167 considered in the statistical model for mortality at population level. At the bottom, the thick black
 168 arrows indicate the relationships considered in the statistical model for the probability of mortality
 169 at individual level (solid lines: expected positive effect; dashed lines: expected negative effect;
 170 nonlinear effects were expected for size, as well as interaction effects between size on the one hand
 171 and all other factors). PLC – percentage of loss of conductance.

172
 173 In this study, we used a combination of statistical regression models, and the PBM CASTANEA
 174 (Figure 1), to investigate patterns of mortality within a population located at the warm and dry
 175 ecological margin for European beech (42° 28' 41" N, 3° 1' 26" E; Supplementary Fig. S1). Mortality,
 176 decline (crown defoliation and fungi presence), size, growth, competition and budburst were
 177 characterised in a set of 4323 adult trees over a 15 year-period from 2002 to 2016. CASTANEA was
 178 used to simulate the number of late frost days (integrating tree phenology), the percentage of loss of
 179 conductance (PLC) and the biomass of carbon reserves in response to stress. Specifically, we
 180 addressed the following issues: (1) When and how do climate variations trigger mortality at
 181 population level; and (2) how do factors varying at tree-level modulate the individual tree's

182 probability of mortality? To answer the first issue, we used CASTANEA simulations at population-level
183 to study the relationship between the simulated response variables and the observed mortality rate.
184 We also tested the impact of climatic variables related to drought duration and intensity on the
185 population-level mortality rate with a beta-regression model. To answer the second issue, we used
186 on the one hand logistic regression to characterise the respective effects of exogenous and
187 endogenous factors on the individual probability of mortality (see detailed expectations on Figure 1),
188 and on the other hand CASTANEA to investigate how differences in tree size, phenology, and
189 defoliation affected the physiological responses to stress.

190 **Materials and Methods**

191 **Study site**

192 La Massane is a forest of 336 ha located in the French eastern Pyrenees ranging from 600 to 1127
193 m.a.s.l. [Located in the south of the beech range](#), the forest is at the junction of Mediterranean and
194 mountainous climates with a mean annual rainfall of 1260 mm (ranging from 440 to 2000 mm) and
195 mean annual temperature of 11°C ([with daily temperature ranging from -10°C to 35°C](#))
196 (Supplementary Fig. S2). No logging operations have been allowed since 1886 and the forest was
197 classified as a reserve in 1974. European beech is the dominant tree in the canopy representing about
198 68% of basal area of the forest. Beech is in mixture with downy oak (*Quercus pubescens* Willd), maple
199 (*Acer opalus* Mill., *Acer campestre* L., *Acer monspessulanum* L.), and holly (*Ilex aquifolium* L.). A 10 ha
200 fenced plot has excluded grazing from cows since 1956. All trees from this protected plot have been
201 geo-referenced and individually monitored since 2002 (Supplementary Fig. S3).

202 We estimated the soil water capacity (SWCa) through soil texture, soil depth and percentage of
203 coarse elements measured in two soil pits. Secondly, we estimated the mean Leaf Area Index (LAI) by
204 using hemispherical photographs (Canon 5D with Sigma 8mm EXDG fisheye). We computed the LAI
205 and clumping index following the methodology described by Davi et al. (2009). [SWCa and LAI were](#)
206 [measured at population level.](#)

207 **Individual tree measurements**

208 This study is based on the characterisation of twelve variables in 4323 beech trees in the
209 protected plot over the period from 2002 to 2016 (Table 1). [Note that beech sometimes produces](#)
210 [stump shoots resulting in multiple stems from a single position \(coppice\)](#), but that here, every stem
211 of all the coppices was individually monitored and subsequently referred to “tree”.

212

213 **Table 1: Quantitative and categorical variables measured at individual level.** All the variables were
 214 measured in 4323 trees, except for H₂₀₀₂ (1199 trees). The “Cat” column indicates both the category
 215 (i.e. size, growth, competition, decline, phenology) and whether it is endogenous (Endo) or
 216 exogenous (Exo). The “YMeas.” column indicates the year of measurement; note that all the variables
 217 were measured only once, so when 2 dates are given they indicate the period over which the variable
 218 is computed.
 219

Quantitative variables measured at individual level							
Code	Variable	Cat	YMeas.	mean	min	max	unit
DBH₂₀₀₂	Diameter at breast height measured in 2002	Size Endo	2002	21.65	10	116	cm
DBH₂₀₁₂	Diameter at breast height measured in 2012	Size Endo	2012	22.84	10	116	cm
MBAI	Mean basal area increment between 2002 and 2012.	Growth Endo	2002- 2012	4.66	0	95	cm ² . year ⁻¹
H₂₀₀₂	Height measured in 2002	Size Endo	2002	8.8	2	26	m
DEFw	Cumulated and weighted defoliation score	Decline Endo	2003- 2016	0.14	0	1	
Nstem	Number of stems observed in the coppice	Compet Exo	2002	1.54	1	11	
Compet_{intra}	Intra-specific competition index	Compet Exo	2002	2.74	0	11.43	
Compet_{intra+}	Intra-specific competition index accounting for within-coppice competition	Compet Exo	2002	1.03	0	12.69	
Compet_{tot}	Total competition index, accounting for within-coppice competition	Compet Exo	2002	4.63	0.12	19.98	
Categorical variables measured at individual level							
Code	Variable	Cat	YMeas.	Level	Number of trees		
Fungi	Presence (1) or absence (0) of the saproxylic fungus	Decline Endo	2003- 2016	1: 0:	414 3913		
Budburst	Early (1) or late (0) budburst	Phenolog y Endo	2002	1 0	237 4090		

220

221

222 Tree mortality was recorded every year from 2003 to 2016, based on two observations (in
223 autumn, based on defoliation and in spring, based on budburst). A tree was considered to have died
224 at year n when (1) budburst occurred in the spring of year n but (2) no leaves remained in the autumn
225 of year n , and (3) no budburst occurred in year $n+1$. All the 4323 trees were alive in year 2003
226 (Supplementary Fig. S4). We computed the annual mortality rate (τ_n) for each year n as:

$$227 \tau_n = \frac{N_{dead,n}}{N_{alive,n-1}} \text{ (Equation 1),}$$

228 where $N_{dead,n}$ (respectively $N_{alive,n}$) is the number of dead (respectively alive) trees in year n .

229 Diameter at breast height (DBH) was measured 1.30 m above ground level in 2002 and 2012.
230 As we focused on the drivers of mature tree mortality, only trees with DBH_{2002} greater than 10 cm
231 were retained for analysis. Individual growth was measured by the mean increment in basal area
232 (MBAI) between 2002 and 2012, estimated as:

$$233 MBAI_i = (\pi(DBH_{2012} - DBH_{2002})^2/4)/N_{yearsAlive_i} \text{ (Equation 2),}$$

234 where $N_{yearsAlive_i}$ is the number of years where individual i was observed being alive. Height
235 in 2002 was estimated for a subset of 1199 trees.

236 A bimodal pattern in budburst phenology had been previously reported in La Massane (Gausson
237 1958; Perci du Sert 1982). Some trees were observed to systematically initiate budburst about two
238 weeks before all the others. Here, the monitoring allowed budburst phenology to be surveyed as a
239 binary categorical variable, distinguishing trees with early budburst from the others.

240 The presence of defoliated major branches was recorded each year between 2003 and 2016
241 (except 2010) as a categorical measure (DEF = 1 for presence; DEF = 0 for absence). These annual
242 measures were cumulated and weighted over the observation period for each individual as:

$$243 DEFw_i = \frac{\sum_{j=1}^{N_{yearsAlive_i}} DEF_j}{N_{yearsAlive_i}} \text{ (Equation 3),}$$

244 Year 2010 was not included in $N_{yearsAlive_i}$. DEFw is an ordered variable integrating (without
245 disentangling) the recurrence of defoliation and the ability to recover from defoliation. The presence
246 of fructification of the saproxylic fungus *Oudemansiella mucida* (Schrad.) was recorded as a
247 categorical measure (Fungi = 1 for presence; Fungi = 0 for absence). Given that once observed, the
248 fructification persists throughout the subsequent years, we analysed it as a binary variable.

249 Competition around each focal beech stem was estimated by the number of stems in the
250 coppice (N_{stem}) as an indicator of within-coppice competition. We also computed competition
251 indices accounting simultaneously for the diameter (DBH_{2002}) and the distance (d_{ij}) of each competitor
252 j to the competed individual i , following Martin and Ek (1984):

253
$$Compet_{i,dmax} = \frac{1}{DBH_{2002i}} \sum_{j=1}^{N_{compet}} DBH_{2002j} \exp \left[\frac{-16d_{ij}}{DBH_{2002i} + DBH_{2002j}} \right] \quad (\text{Equation 4}),$$

254 where N_{compet} is the total number of competitors in a given radius d_{max} (in m) around each focal
255 individual i . Only trees with $DBH_{2002j} > DBH_{2002i}$ are considered as competitors. Such indices were
256 shown to describe more accurately the competition than indices relying on diameter only (Stadt et
257 al. 2007). We computed this competition index in three ways. The intra-specific competition index
258 $Compet_{intra}$ only accounts for the competition of beech stems not belonging to the coppice of the
259 focal tree. The intra-specific competition index $Compet_{intra+}$ accounts for all beech stems belonging,
260 or not, to the coppice of the focal tree. The total competition index $Compet_{tot}$ accounts for all stems
261 and species. We considered that stems located less than 3 m away from the focal stem belonged to
262 the same coppice. The three indices were first computed at all distances from 1 m (or 3 m for
263 $Compet_{intra}$) to 50 m from the target tree, with 1 m steps. We then retained $d_{max} = 15$ m in subsequent
264 analyses, because all indices reached a ceiling after this distance value, suggesting that in a radius
265 greater than 15 m, the increasing number of competitors is compensated for by distance.

266 Climate data

267 Local climate has been daily monitored *in situ* since 1976 and 1960 for temperature and
268 precipitation/mean relative humidity, respectively. In order to obtain a complete climatic series (from
269 1959 to 2016), we used the quantile mapping and anomaly method in the R package “meteoland”
270 (De Caceres et al. 2018), considering the 8-km-resolution-SAFRAN reanalysis (Vidal et al. 2010) as
271 reference.

272 From the corrected climate series, we derived the daily climatic input variables for CASTANEA,
273 which are the minimum, mean and maximum temperatures (in °C), the precipitation (mm), the wind
274 speed ($m \cdot s^{-1}$), the mean relative humidity (%) and the global radiation ($MJ \cdot m^{-2}$). We also computed
275 two standardised precipitation-evapotranspiration indices (SPEI), varying between -2 (indicating
276 aridity) and 2 (indicating wetness), using the R package “SPEI” (Beguería and Vicente-Serrano 2017).
277 The cumulated SPEI from June to August with a three-month buffer (SPEI3_JJA) was used as an
278 indicator of average drought level during the vegetative season. The lowest monthly SPEI-value over
279 the vegetative season (SPEI1_dryVg) was used as an indicator of drought intensity (see Appendix 1
280 for details).

281 Simulations with CASTANEA

282 **Model overview:** CASTANEA is a PBM initially developed to simulate carbon and water fluxes in forest
283 ecosystems with no spatial-explicit representation of trees (Dufrêne et al. 2005). A tree is abstracted

284 as six functional elements: leaves, branches, stem, coarse roots, fine roots and reserves
285 (corresponding to non-structural carbohydrates). The canopy is divided into five layers of leaves.
286 Photosynthesis is half-hourly calculated for each canopy layer using the model of Farquhar et al.
287 (1980), analytically coupled to the stomatal conductance model proposed by Ball et al. (1987).
288 Maintenance respiration is calculated as proportional to the nitrogen content of the considered
289 organs (Ryan 1991). Growth respiration is calculated from growth increment combined with a
290 construction cost specific to the type of tissue (De Vries, Brunsting, and Van Laar 1974). Transpiration
291 is hourly calculated using the Monteith (1965) equations. The dynamics of soil water content (SWCo;
292 in mm) is calculated daily using a three-layer bucket model. Soil drought drives stomata closure via a
293 linear decrease in the slope of the Ball et al. (1987) relationship, when relative SWCo is under 40% of
294 field capacity (Granier, Biron, and Lemoine 2000; Sala and Tenhunen 1996). In the carbon allocation
295 sub-model (Davi et al., 2009; Davi & Cailleret 2017), the allocation coefficients between
296 compartments (fine roots, coarse roots, wood, leaf and reserves) are calculated daily depending on
297 the sink force and the phenological constraints. CASTANEA model was originally developed and
298 validated at stand-scale for beech (Davi et al. 2005).

299 **Focal processes and output variables:** In this study, we focussed on three response variables
300 simulated by CASTANEA: (1) the biomass of reserves (BoR) as an indicator of vulnerability to carbon
301 starvation, (2) the percentage of loss of conductance (PLC) as an indicator of vulnerability to hydraulic
302 failure, and (3) the number of late frost days (NLF) as an indicator of vulnerability to frost damage.
303 Note that we did not simulate mortality with CASTANEA because the thresholds in PLC, NLF and BoR
304 triggering mortality are unknown. These variables were simulated using the CASTANEA version
305 described in Davi and Cailleret (2017) with two major modifications. First, for budburst, we used the
306 one-phase UniForc model, which describes the cumulative effect of forcing temperatures on bud
307 development during the ecodormancy phase (Chuine, Cour, and Rousseau 1999; Gauzere et al. 2017).
308 We simulated damage due to late frosts (see details in Appendix 2) and considered that trees were
309 able to reflush after late frosts. We calculated NLF as the sum of late frost days experienced after
310 budburst initiation.

311 Second, we implemented a new option in CASTANEA to compute PLC following the Pammenter
312 and Willigen (1998) formula:

$$313 \quad PLC = \frac{1}{1 + e^{slope(\Psi_{leaf} - \Psi_{P50})}} \quad (\text{Equation 5}),$$

314 with Ψ_{leaf} (MPa) the simulated midday leaf water potential, Ψ_{50} (MPa) the species-specific
315 potential below which 50% of the vessels are embolized, and *slope* a constant fixed to 50.

316 The leaf water potential Ψ_{leaf} was calculated as:

$$\begin{aligned} \Psi_{leaf}(t+1) &= \Psi_{soil}(t+1) - \frac{TR}{3600} \times R_{SoilToLeaves} + \frac{\Psi_{leaf}(t)}{\Psi_{soil}(t+1) + TR \times R_{SoilToLeaves}} \\ &\times e^{\frac{\Delta T}{R_{SoilToLeaves} \times Cap_{SoilToLeaves}}} \end{aligned}$$

(Equation 6)

where the soil water potential (Ψ_{soil} MPa) was calculated from daily SWCo (Campbell 1974). Ψ_{leaf} was calculated hourly ($\Delta T = 3600s$) based on the sap flow (TR in $mmol \cdot m^{-2} \cdot leaf^{-1}$) simulated following the soil-to-leaves hydraulic pathway model of Loustau et al. (1990). We used a single resistance ($R_{SoilToLeaves}$ in $MPa \cdot m^{-2} \cdot s^{-1} \cdot kg^{-1}$, following Campbell 1974) and a single capacitance ($Cap_{SoilToLeaves}$ in $kg \cdot m^{-2} \cdot MPa^{-1}$) along the pathway. $R_{SoilToLeaves}$ was assessed using midday and predawn water potentials found in the literature.

We added a binary option in CASTANEA to simulate branch mortality and defoliation as a function of PLC. If the PLC at year n was >0 , the LAI at year n was reduced by the PLC value for trees able to defoliate (option “Defoli-able”). Otherwise, PLC has no consequences on LAI.

Simulation design: The aim of the first simulations was to investigate whether response variables simulated by CASTANEA correlated with patterns of observed mortality at population scale. We simulated a population of 100 trees representing the variability in individual characteristics observed in La Massane in terms of height-diameter allometry, DBH, leaf area index and budburst phenology (Appendix 2). We also simulated a range of environmental conditions representing the observed variability in SWCa and tree density. CASTANEA was validated based on ring width patterns (Appendix 2). Values of focal output variables (PLC, NLF and BoR) were then averaged across the 100 trees. We also computed a composite vulnerability index (CVI) for each year n combining the simulated PLC, NLF and BoR as follows:

$$CVI_n = \left(\frac{PLC_n}{\max(PLC)} + \frac{NLF_n}{\max(NLF)} \right) - \frac{BoR_n}{\max(BoR)} \quad (\text{Equation 7}),$$

Note that each term is weighted by its maximal value across all years, so that the contribution of the three drivers to vulnerability is balanced. The possible range of CVI is $[-1; 2]$.

The second simulation aimed at investigating the differences in physiological responses between individuals with different characteristics. We simulated eight individuals corresponding to a complete cross design with two size categories (5 and 40 cm in DBH), two budburst types (early and normal), and two defoliation levels (option “Defoli-able” activated or not).

Statistical models of mortality

Population-level: We used a beta-regression model to investigate the effects of climate on annual mortality rate at population-level. Beta-regression models predict a response variable varying

348 between [0; 1] and account for features like heteroscedasticity or asymmetry, which are commonly
349 obtained in time-series of annual mortality rates. We investigated the following model for mortality
350 at year n (with n varying from 2004 to 2016):

$$351 \quad \tau_n = \text{SPEI1_dryVg}_n \times \text{SPEI3_JJA}_n \text{ (Equation 8),}$$

352 where SPEI1_dryVg is lowest monthly value of SPEI during the vegetative season; and SPEI3_JJA is
353 cumulated SPEI from June to August computed over three months. As the number of observations
354 (years) was low, we focussed on these two predictors expected to cause mortality based on beech
355 ecology (Bréda et al. 2006).

357 Beta-regression was fitted with the R package 'betareg' (Cribari-Neto and Zeileis 2010). **The**
358 **variables were scaled before fitting the model.** Model validity was checked based on the leverage
359 points (i.e. points having a greater weight than expected by chance) with the Cook's distance (Cook
360 distance < 0.5 indicate no leverage). We evaluated the goodness-of-fit with the Brier test score (Brier
361 1950). We evaluated the sensitivity and specificity of the model using the receiver operating
362 characteristic (ROC) curve.

363 **Individual-level:** We used logistic regression models to investigate how tree characteristics affect the
364 individual probability of mortality ($P_{\text{mortality}}$). This approach is appropriate for a binary response
365 variable and a mixture of categorical and quantitative explanatory variables, which are not necessarily
366 normally distributed (Hosmer and Lemeshow 2000). We considered the following complete logistic
367 regression model:

$$368 \quad P_{\text{mortality}} = [\text{DEFw} + \text{Fungi} + \text{Budburst} + \text{MBAI} + (\text{Nstem OR Compet}_{\text{intra}} \text{ OR Compet}_{\text{intra}} \text{ OR} \\ 369 \quad \text{Compet}_{\text{tot}})] \times (\text{DBH}_{2002} + \text{DBH}_{2002}^2) \text{ (Equation 9)}$$

370 where the predictors defoliation (DEFw), growth (MBAI), size (DBH_{2002}) and competition (Nstem or
371 the Compet indices) were quantitative variables, and the presence of fungi (Fungi) and budburst
372 phenology (Budburst) were categorical variables. We included both a linear and quadratic effect of
373 DBH_{2002} by specifying this effect as a polynomial of degree 2. Interaction effects of the previous
374 predictors with this polynomial were included.

375 **All variables were scaled before fitting the model.** To select the best competition-related
376 variables, we first fitted the model described by equation 9 with each competition term successively
377 (Appendix 3). Then, we used a stepwise procedure to select the most parsimonious model based on
378 AIC. When two models had similar AIC ($\Delta < 2$) (Arnold 2010), the one with fewer variables (most
379 parsimonious) was selected. Model validity and fit quality were checked using similar tools as for the
380 beta-regression model.

381 Collinearity resulting from correlations between predictor variables is expected to affect the
382 statistical significance of correlated variables by increasing type II errors (Schielzeth 2010). To
383 evaluate this risk, we first checked for correlation among predictors included in equation 9 (Fig. S5).
384 We also computed the variation inflation factor (VIF) with the R package “car”. A threshold of VIF < 4
385 is commonly accepted to show that variables are not excessively correlated and do not render the
386 model unstable.

387 We expressed the results in terms of odds ratios, also called relative risk, indicating the degree
388 of dependency between variables. For instance, the odds ratio for mortality as a function of budburst
389 characteristics (early or normal) is:

$$390 \quad \text{Oddsratio}_{\text{EarlyvsNormal}} = \frac{\text{Odds}_{\text{Early}}}{\text{Odds}_{\text{Normal}}} \quad (\text{eq 10}),$$

$$391 \quad \text{With } \text{Odds}_{\text{Early}} = \frac{P_{\text{mortality}}(\text{Early})}{1 - P_{\text{mortality}}(\text{Early})} \text{ and } \text{Odds}_{\text{Normal}} = \frac{P_{\text{mortality}}(\text{Normal})}{1 - P_{\text{mortality}}(\text{Normal})}.$$

392 We computed odds ratios with “questionr” the R package (Barnier, Briatte, and Larmarange 2018).
393 The interactions were visualized with the package “jtools” (Long 2018).

394 Results

395 Population-level patterns of mortality

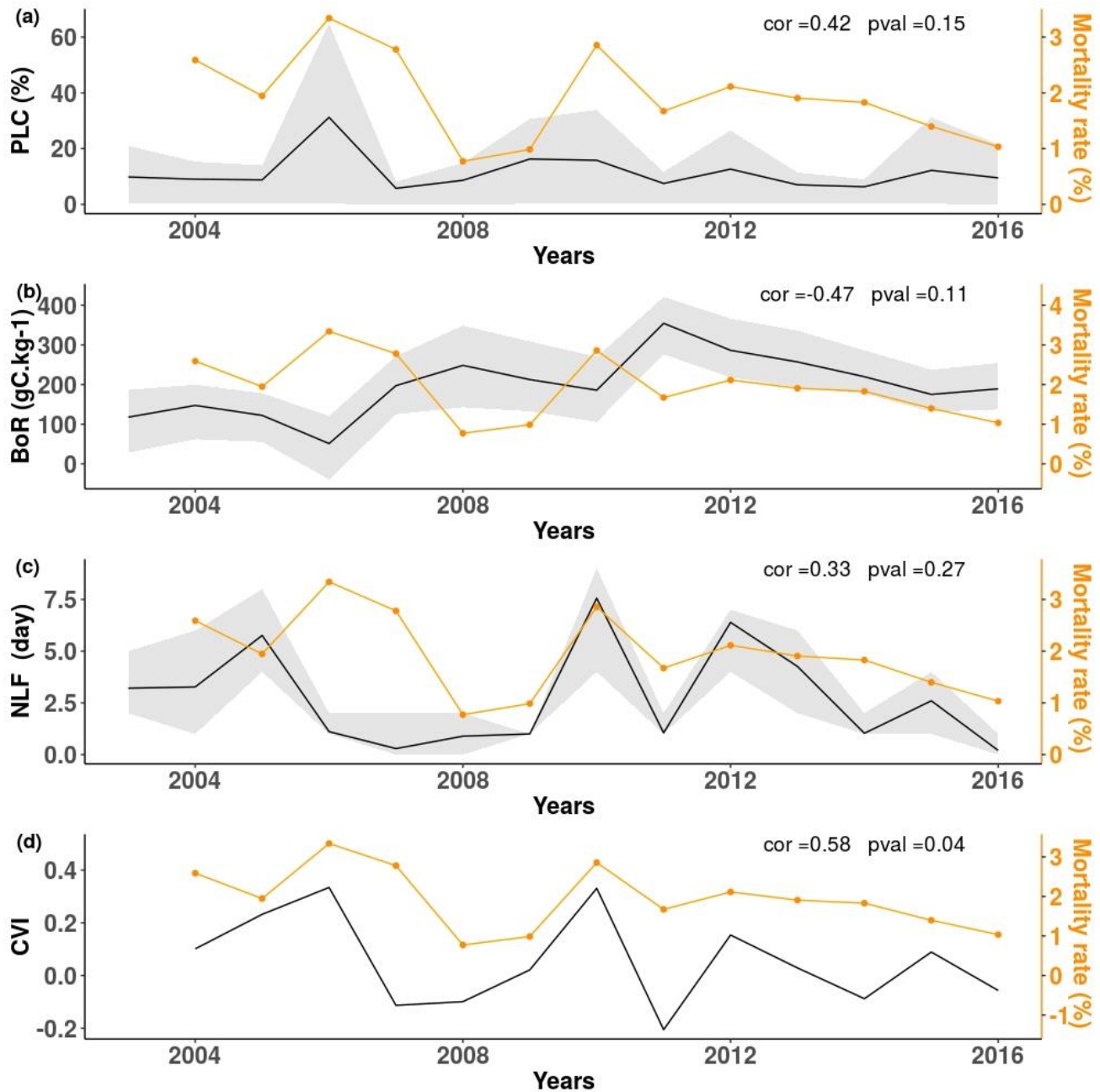
396 The total mortality rate between 2004 and 2016 was 23% (Figure 2; Table S1). After 2004 (2.6%),
397 two peaks of high mortality were observed, in 2006-2007 (3.3% in 2006) and in 2010 (2.9%). The
398 lowest mortality rate was observed in 2008 (0.8%).

399 CASTANEA simulated inter-annual variations in the PLC: the mean PLC value varied among
400 years, from 1% in 2004 and 2005 to 31% in 2006 (Fig. 2a). The mean simulated biomass of carbon
401 reserves (BoR) varied among years, from 51 gC.m⁻² in 2006 to 354 gC.m⁻² in 2011. Finally, the number
402 of late frost days (NLF) varied among years, from 0.2 in 2016 to 7.56 days in 2010 (Fig. 2c). The
403 variation in the composite vulnerability index (CVI) integrated these different responses (Fig. 2d),
404 showed a peak in 2006 (drought), in 2010 (late frost) and in 2012 (combination of frost and drought).

405 None of the response variables simulated by CASTANEA (NLF, PLC, BoR) was significantly
406 correlated to annual variation in mortality rate. The only significant correlation was observed
407 between CVI and the annual mortality rate ($r = 0.58$, $p\text{-value} = 0.04$). Hence, inter-annual variations
408 in CVI were a good predictor of the mortality rate, except in year 2007.

409

410 **Figure 2: Stress-related output variable simulated with CASTANEA from 2004 to 2016: (a)**
411 **percentage of loss of conductance (PLC); (b) biomass of reserves in gC.kg⁻¹ (BoR); (c) number of late**
412 **frost days (NLF); (d) Composite vulnerability index (CVI) integrating a+b+c.** The black line is the
413 mean of simulation, and the grey area represents the inter-individual variation from the 1st to the 3rd
414 quartile. The yellow line is the mortality rate observed in La Massane.
415



416

417

418 The beta-regression model revealed a significant impact of climate variables on the observed
 419 mortality rate at population-level (Appendix 1). SPEI1_dryVg, SPEI3_JJA and their interactions
 420 explained 32% of the variation in mortality rate between years. This model had both fair validity and
 421 goodness-of-fit. For low values of SPEI3_JJA (i.e. during dry summers), mortality increased with
 422 decreasing SPEI1_dryVg (i.e., increasing drought intensity). However, non-expected interaction
 423 effects were observed for high values of SPEI3_JJA (i.e. during wet summers), where mortality
 424 increased with increasing SPEI1_dryVg (i.e., decreasing drought intensity).

425 **Statistical model of mortality at individual level**

426 **Table 2: Effects of variables varying at tree-level on the individual tree's probability of mortality.**
 427 Variables are defined in Table 1. Effects were estimated with a logistic regression model (equation 9).
 428 β is the maximum likelihood estimate, with its estimated error (SE), z-value, and associated p-value.
 429 OR is the odds ratio.
 430

Variables	β	SE	z value	p-value	OR
DEFw	6.91	0.26	26.29	< 2.2 e-16	1.0 e03
DBH₂₀₀₂	-11.59	5.15	-2.25	2.42 e-02	9.22 e-06
DBH₂₀₀₂²	22.25	4.95	4.50	6.86 e-06	4.60 e09
MBAI	-5.91e-02	1.06 e-02	-5.55	2.80 e-08	0.94
Budburst	0.81	0.17	4.69	2.69 e-06	2.25
Nstem	0.12	3.60 e-02	3.42	6.24 e-04	1.13
Fungi	0.56	0.14	3.94	8.10 e-05	1.75
DEFw:poly(DBH₂₀₀₂)1	-55.17	14.81	-3.73	1.95 e-04	1.10 e-24
DEFw:poly(DBH₂₀₀₂)2	32.09	16.81	1.91	5.63 e-02	8.64 e13
poly(DBH₂₀₀₂)1:MBAI	0.37	0.45	0.83	0.41	1.45
poly(DBH₂₀₀₂)2:MBAI	-0.83	0.44	-1.89	5.90 e-02	0.43

431
 432 All the variables listed in equation 9 were retained in the best model and had a significant main
 433 effect on the probability of mortality (Table 2). This model explained 49% of the observed mortality
 434 and had both a high validity and goodness-of-fit (Appendix 3). **Defoliation had the strongest linear**
 435 **effect on mortality: the relative probability of mortality increased by 1000 times for a one-unit**
 436 **increase in DEFw**. Then, the probability of mortality was 2.25 higher for trees with earlier budburst as

437 compared to others, and 1.75 higher for trees bearing fungi fructifications as compared to others.
438 Among the competition-related variables, N_{stem} was selected as it was associated with the lowest AIC.
439 The probability of mortality increased with increasing N_{stem} , and decreased with increasing MBI.
440 Regarding the effect of tree size, the polynomial of degree 2 corresponded to a U-shape and traduced
441 a higher relative probability of mortality for both the smaller and the larger trees (Table 3, Appendix
442 3).

443 Interaction effects between size and defoliation on mortality were significant: the probability
444 of mortality increased more rapidly with DEFw for small rather than larger trees, and at an equal level
445 of defoliation, the probability of mortality was always higher for smaller trees (Fig. 3a, Table 2).
446 Interaction effects between size and growth on mortality were also significant: [the decrease in the](#)
447 [probability of mortality with increasing mean growth was evident mostly for small trees \(Fig. 3b\).](#)
448 These results were robust for the choice of the competition variable (N_{stem} versus competition
449 indices), for the choice of the size variable (height instead of diameter) and for the consideration of
450 size (DBH_{2002}) as a quantitative versus categorical variable (Appendix 3). [Finally, we obtained](#)
451 [convergent results with an alternative approach \(survival analysis\) which account simultaneously for](#)
452 [both levels of variability \(individual and temporal\) in our data set \(Appendix 4\).](#)

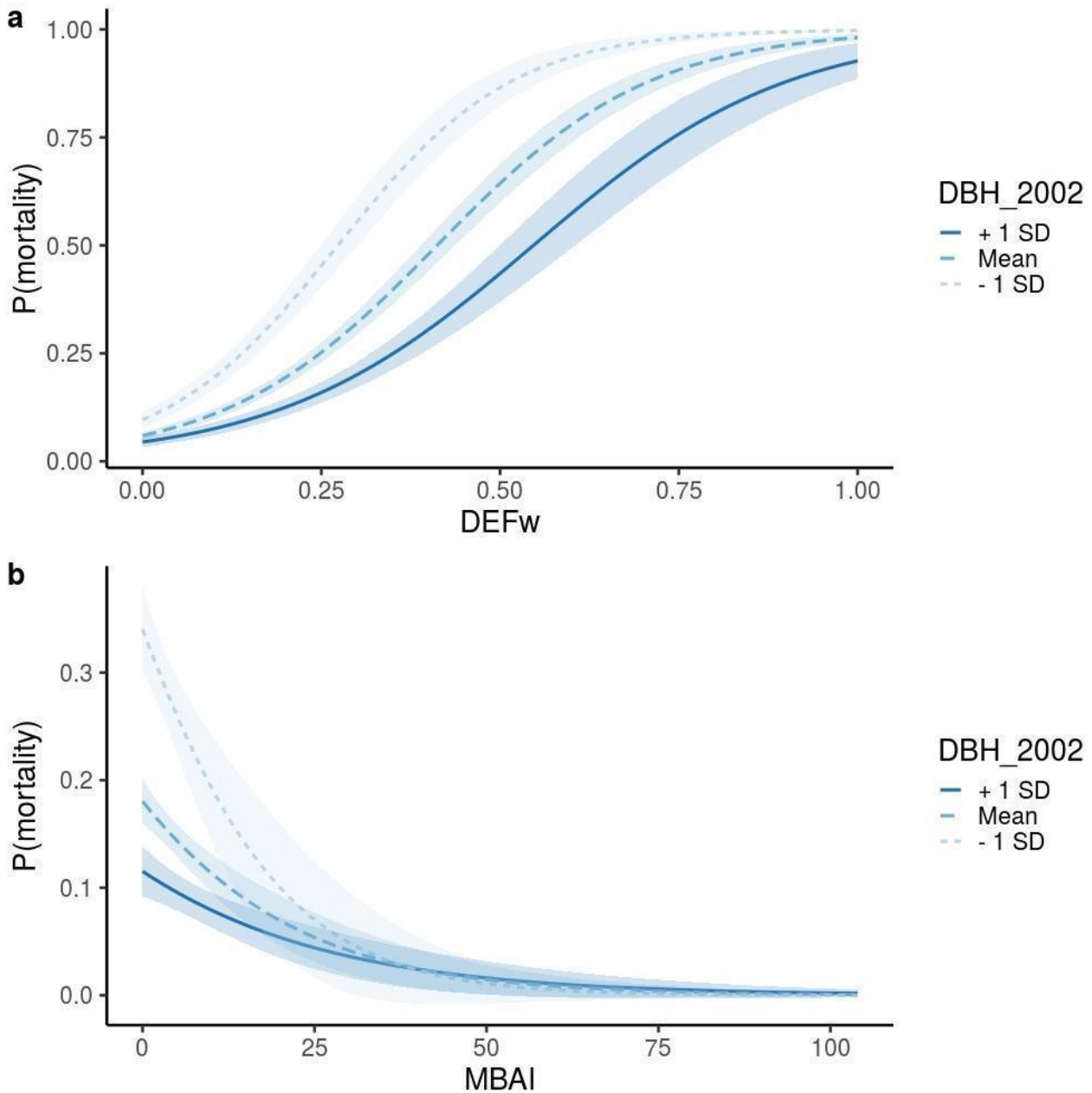
453 Process based model at individual scale

454 Simulations with CASTANEA showed that inter-individual differences in tree size, phenology,
455 and defoliation, together with the intensity of climatic stress, affected the physiological responses to
456 stress. [The magnitude of the individual effects on tree vulnerability differed during a drought year](#)
457 [\(2006\), a frost year \(2010\) and a good year \(2008, 2014 or 2016\) \(Fig. 4\).](#) The loss of conductance was
458 higher for trees with early budburst and for larger trees, but this effect was only evident in drought
459 years (Fig. 4a). Moreover, during drought, the ability to defoliate decreased the risk of cavitation (Fig.
460 4a) but increased the risk of carbon starvation (Fig. 4b). By contrast, phenology only poorly affected
461 the biomass of reserve (BoR): even during a frost year, trees with earlier budburst did not reduce
462 their BoR, due to their ability to reflush (Fig. 4b). BoR was always lower for large tree, even without
463 stress. This was to be expected, [because there is no explicit competition for light in CASTANEA. Hence](#)
464 [large trees and small trees have a relatively similar photosynthesis when it is scaled by soil surface](#)
465 [\(large trees photosynthesize slightly more because they have a stronger LAI\). Large trees, on the other](#)
466 [hand, have a larger living biomass and thus a higher level of respiration, which leads to lower reserves.](#)

467

468

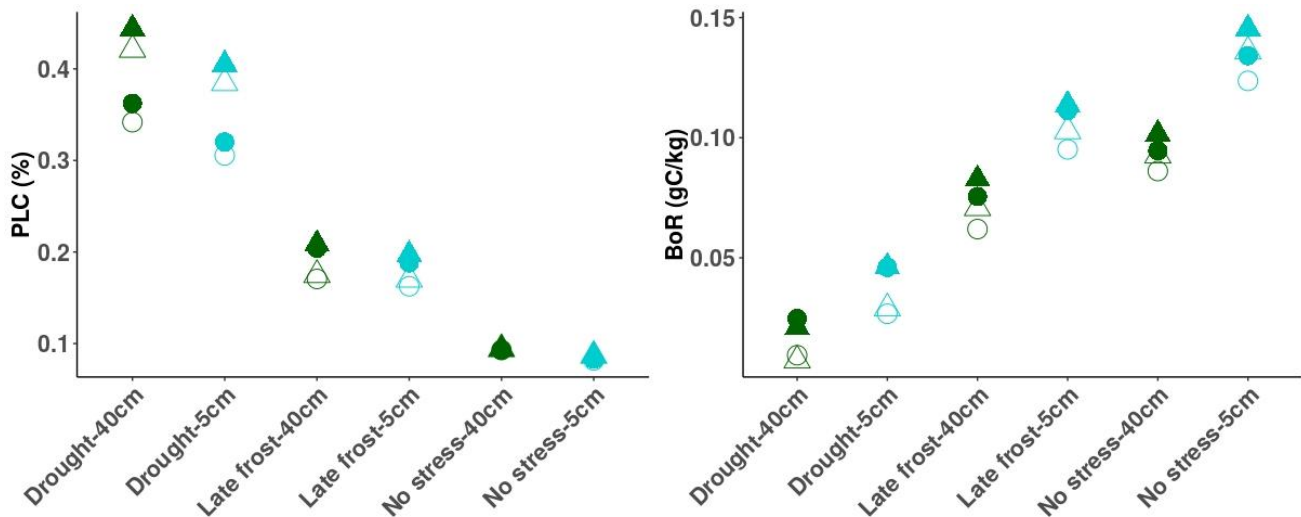
469 **Figure 3: Interaction effects in the logistic regression model at individual-level** (a) between diameter
470 (DBH₂₀₀₂) and weighted defoliation (DEFw). (b) between DBH₂₀₀₂ and the mean growth in basal area
471 (MBAI). Regression lines are plotted for three values of DBH₂₀₀₂, corresponding to ± 1 standard
472 deviation (10.7 cm) from the mean (22 cm). Confidence intervals at 95% are shown around each
473 regression line.



474
475

476

477 **Figure 4: Physiological proxies of vulnerability simulated for eight trees differing in size, defoliation**
478 **and budburst phenology.** We focus on three key years: 2006 (drought); 2008 (no stress); 2010 (late
479 frosts). Colours indicate the DBH at the beginning of the simulation: 5 cm (light blue) versus 40 cm
480 (dark green). Triangles (respectively round) indicate individuals with early (respectively “normal”)
481 budburst. Empty (respectively full) indicate individuals able (respectively not able) to defoliate.
482



483

484 Discussion

485 By combining statistical and process-based models at population and tree-level (Figure 1), this
486 study shed new lights on when and how climate variations trigger mortality and how factors varying
487 at tree-level modulate the individual vulnerability to drought and frost stresses (Table S2).

488 Increasing population-level rate of mortality in response to drought and frost

489 The annual mortality rates observed in this study ranged between 0.7 and 3.3% (mean value =
490 2%). This is at the upper range of the few mortality estimates available for beech. Hülsmann et al.
491 (2016) reported annual mean rates of mortality of 1.4%, 0.7% and 1.5% in unmanaged forests of
492 Switzerland, Germany and Ukraine, with a maximum mortality rate of 2.2%. Archambeau et al. (2019)
493 estimated even lower mortality rates (mean annual value = $3.8 \times 10^{-3}\%$, range = $3.7 \times 10^{-3}\%$ to $3.8 \times 10^{-3}\%$)
494 from European forest inventory data (including managed and unmanaged forests). Overall, these
495 mortality rates are low when compared to other tree species; for instance, according to the French
496 national forest inventory, the average mortality is 0.1% for beech against 0.3% on average for other
497 species and 0.4% for spruce or 0.2% for silver fir (IFN 2016). The relatively high value observed here
498 may result from the absence of management, combined with the population location being at the
499 dry, warm margin of species distribution (Fig. S1), where most population extinctions are expected in
500 Europe (Thuiller et al. 2005). However, we cannot rule out that these different mortality estimates

501 are also affected by the size threshold in inventories, which differ between studies (including smaller
502 trees automatically increases the mortality rate).

503 We showed that inter-annual variations in the observed mortality rate at population-level were
504 significantly associated with variations in the composite vulnerability index (CVI) integrating the
505 number of late frost days (NLF), the percentage of loss of conductance (PLC) and the biomass of
506 carbon reserves (BoR) simulated by CASTANEA. This association was not found when the three
507 response variables simulated by CASTANEA were considered separately, highlighting that patterns of
508 mortality in beech are driven by a combination of drought, and late-frost, stresses. In particular,
509 simulations showed that in 2010 (a year without drought), the high mortality rate coincided with an
510 extreme late frost event. This is consistent with the study of Vanoni et al (2016), which showed that
511 both drought and frost could contribute to beech mortality. These results are also consistent with the
512 emerging consensus that mortality at dry, warm margins is not due either to carbon starvation or
513 hydraulic failure, but is rather the result of a balance of all these responses (e.g. McDowell et al. 2011;
514 Sevanto et al. 2014).

515 This study also found a significant relationship between the observed mortality rate and SPEI
516 variables computed from climatic series. A major role of SPEI on mortality has already been found by
517 Archambeau et al. (2019) in beech, by Davi and Cailleret (2017) in silver fir, or by Carnicer et al., (2011)
518 in 12 European tree species. Here, the statistical regression model including only SPEI variables
519 suggested that mortality was triggered by summer droughts, including both the pulse effects of
520 severe drought (through SPEI1_dryVg) but also long-term effects of repeated droughts (through
521 SPEI3_JJA). Our results additionally suggest an interaction between long-term and pulse effects of
522 drought on mortality i.e. the risk of mortality increased more than the sum of risks predicted by each
523 factor separately. However, the biological interpretation of some of these interaction effects was not
524 evident. This may be due to the low number of observations, with only 14 years in the mortality
525 survey. This may also confirm that integrative measurements of the response to stresses, such as the
526 CVI proposed here, allow a better understanding of when and how mortality occurs than purely
527 stress-related climatic variables.

528 In future developments, the CVI could be refined in several ways. Its different components
529 could be weighted based on ecophysiological knowledge. The CVI could also benefit from taking into
530 account the temporal dynamics of mortality, such as the existence of positive or negative post-effects
531 across years. The low number of observations in this study compelled us not to account for these
532 lagged effects, which probably explains why the CVI failed to predict the high mortality observed in
533 2007. Indeed, the high mortality of 2007 is probably due to the lagged effect of the 2006 drought.

534 [Such lags between the weakening of a tree and its final death were shown for beech in Vanoni \(2016\)](#)
535 [and silver fir in Davi & Cailleret \(2017\).](#)

536 Inter-individual variation in the vulnerability to drought and frost

537 The large number of trees individually monitored in this study provided us with an exceptionally
538 large sample size to test for the effects of factors modulating individual vulnerability to drought and
539 frost in beech. [Firstly, we found that a higher mean growth was associated with a lower probability](#)
540 [of mortality, as previously demonstrated \(Cailleret and Davi 2011; Gao et al. 2018\).](#) This decrease in
541 [mortality with increasing mean growth was evident mostly for small trees as already reported in](#)
542 [beech seedlings \(Collet and Le Moguedec 2007\) and other species \(Kneeshaw et al. 2006; Lines,](#)
543 [Coomes, and Purves 2010\), but not in adult beech trees to our knowledge.](#)

544 Secondly, we found that increased defoliation was associated with increasing mortality. This
545 result was expected from previous studies (Dobbertin and Brang 2001, Carnicer et al. 2011), although
546 the consequences of defoliation are still being debated for beech. Senf et al. (2018) showed that
547 defoliation was associated with tree decline, while Bauch et al., (1996) and Pretzsch (1996) found that
548 the growth of highly defoliated beech trees did not decrease and could even increase in some cases.
549 [Our simulations comparing trees able, or not able, to defoliate, shed light on the multiple effects of](#)
550 [defoliation on mortality.](#) This was achieved by showing that defoliation indeed decreased carbon
551 reserves in good years but could also limit the loss of hydraulic conductance during dry years. We also
552 observed a significant interaction between defoliation and tree size on mortality, showing that small
553 trees were more vulnerable to mortality in response to defoliation than large trees. However, we
554 cannot rule out that this effect is due in part to the categorical method used to survey defoliation,
555 which does not take into account the percentage of crown loss. Hence, defoliation may be biased
556 with respect to size, such that small and defoliated trees will on average have a higher proportion of
557 canopy loss, and therefore be more impacted than large and defoliated trees.

558 Thirdly, both statistical and process-based approaches found that trees with early budburst
559 were more [prone to die](#). By contrast, Robson et al. (2013) showed that trees with early budburst were
560 not more vulnerable to mortality, but rather grew better, consistent with our simulations where trees
561 with early budburst accumulate more reserves during good years. This discrepancy may be due to the
562 location of our studied population at the rear-edge of beech distribution, where earlier budburst
563 dates are observed due to higher temperature and may expose trees to a higher risk of late frost. It
564 may be that the presence of trees with very early budburst in the studied population makes it
565 somewhat unusual, although similar cases have been observed elsewhere (Gausson 1958; Perci du

566 Sert 1982). In CASTANEA simulations, the higher vulnerability of early trees resulted rather from a
567 higher risk of hydraulic failure than a higher impact of late frosts. This is because trees with early
568 budburst have a longer vegetation season and they develop their canopies faster, which also
569 mechanically increases their water needs. Altogether, the relationships between phenology and
570 mortality deserve further investigation, especially since the spatio-temporal variation of budburst
571 patterns under climate change may produce complex spatio-temporal patterns of stresses (Vanoni et
572 al. 2016).

573 Regarding the effect of size, the results differed between the statistical approach, where large
574 trees died less than small ones, and the simulations, which predicted a greater vulnerability to
575 drought of large trees. There may be several explanations for this discrepancy. The first reason is that
576 CASTANEA simulates an average tree without explicit competition for light and water; hence not
577 accounting for the higher observed background mortality in small trees as compared to large ones
578 (Figure S7). In addition, CASTANEA also does not account for individual dominance status, which can
579 affect the current carbon balance of a tree and hence its capacity to mitigate stress. In the studied
580 population, large trees are more likely to be dominant, with better access to light resources
581 promoting carbon accumulation, as compared to small trees, which are more likely to be suppressed.
582 Another reason is that tree size may vary with environmental factors in the studied population, such
583 that large trees have a tendency to occur on better soils. Therefore, the size effect observed through
584 the statistical approach may reveal the confounding effect of spatial soil heterogeneity, not taken
585 into account in the PBM. A measurement of water availability at individual tree level would be
586 necessary to address this issue but was out of the scope of this study.

587 Combining statistical and process-based approaches to identify the causes of tree 588 vulnerability

589 These two approaches illustrate the classical compromise between a fine understanding of
590 physiological mechanisms driving mortality, with complex and expensive PBMs, versus high precision
591 local mortality predictions, with statistical models requiring less data, but having a weaker ability to
592 generalize. Most often, studies adopt either of the two approaches, and generally statistical
593 approaches prevail (Hülsmann et al. 2016; Seidl et al. 2011). However, the two approaches are highly
594 complementary, and combining them allows the deciphering of the respective roles of the drivers
595 and mechanisms underlying tree mortality and understanding their variability among individuals or
596 years (Hawkes 2000; O'Brien et al. 2017; Seidl et al. 2011). The two approaches can be simply
597 compared as done in this study at the individual level, or they can be more finely integrated as done
598 when we analysed the correlation between the observed mortality rate and the simulated variables

599 related to the response to stress. An upper level of integration would be inverse modelling, where
600 observed mortality rates could be used to infer the physiological thresholds (e.g. in BoR, PLC and NLF)
601 likely to trigger mortality (Davi & Cailleret 2017).

602 This study also illustrated a classical difficulty in combining statistical and process-based
603 approaches, related to the difference between observed variables and PBM parameters. For instance,
604 the comparison of defoliated and non-defoliated trees does not have exactly the same meaning when
605 using CASTANEA and the statistical approach. In CASTANEA, we compared trees, able versus unable,
606 to defoliate, while these average trees share on average the same edaphic conditions. In the statistical
607 approach, we compared trees with different levels of defoliation, but which also probably did not
608 share the same edaphic and biotic conditions: Defoliation was thus also likely to be an indicator of
609 the fertility of the environment, such that on shallow soils, defoliation was stronger and the
610 probability of mortality increased. Hence, the correlation does not necessarily involve a causal
611 relationship between defoliation and mortality.

612 The major benefits of our approach combining different approaches (statistical, process-based)
613 at different scales (population, individual) is that it allows us to disaggregate ecological patterns
614 observed at an upper scale (population, multi-year period), and get back to patterns observed at a
615 lower scale where processes operate (individual, year). This ability to aggregate/disaggregate
616 patterns is acknowledged as a powerful approach to understand apparent contradictions between
617 patterns observed at different scales (Clark et al. 2011). There are however some limitations to the
618 approaches we used here. First, none of them could fully account for the non-independence of
619 climatic effects on mortality between years. Indeed, the effect of climatic variables at a given year
620 may depend on other variables expressed in previous years. This was observed in beech, where
621 several drought years finally led to a growth decline (Jump et al. 2006; Knutzen et al. 2017; Vanoni et
622 al. 2016) or a modification in sap flow (Hesse et al. 2019). Moreover, the processes driving mortality
623 may change through time as the most sensitive individuals are progressively eliminated, and/or the
624 surviving trees become less and less sensitive (i.e. acclimation Niinemets 2010). Finally, the statistical
625 model at the individual level could not fully make use of the repeated measurements of mortality
626 over the years, partly because other individual variables were measured only once over the study
627 period (except defoliation). Survival analyses could unfortunately not fully address this limitation
628 (Appendix 4), and the development of a finely tuned Bayesian approach was out of the scope of this
629 study. Besides methodological improvements, another extension to the present study would be to
630 combine statistical and process-based approaches at a larger spatial scale, among populations across
631 climatic gradients. This would allow the investigation of whether the respective drought and late frost

632 sensitivity differ between the rear, core and leading edge of species distribution, as suggested by
633 Cavin and Jump (2017).

634 **Data accessibility**

635 The data set analysed in this preprint is available online under the zenodo repository
636 (<https://doi.org/10.5281/zenodo.3519315>). Raw data can be obtained from JG, JAM and CH.

637 **Supplementary material**

638 The process-based model CASTANEA is an open-source software available on capsis website:
639 <http://capsis.cirad.fr/>
640 Supplementary materials (Figures and Tables) for this preprint are available on bioRxiv (XXX).

641 **Author Contributions**

642 JAM, JG, CH and EM measured and mapped all the trees. CP performed the wood core analyses. CP,
643 FL and SOM designed and ran the statistical models. CP and HD ran the PBM. CP drafted the
644 manuscript, and all authors contributed to its improvement.

645 **Acknowledgments**

646 We are grateful to M. Cailleret, B. Fady, and N. Martin Saint Paul for discussions and comments on a
647 previous version of this manuscript. We thank N. Mariotte for wood core sampling, and F. Guibal for
648 their analyses. SOM and HD were funded by the EU ERA-NET BiodivERsA projects TIPTREE
649 (BiodivERsA2-2012-15) and the ANR project MeCC (ANR-13-ADAP-0006). CP received funding from
650 the European Union's Horizon 2020 research and innovation programme under grant agreement No.
651 676876 (GenTree).

652 **Conflict of interest disclosure**

653 The authors of this preprint declare that they have no financial conflict of interest with the content
654 of this article. SOM is one of the PCIEcology recommenders.

655 **References**

656 Adams, Henry D. et al. 2017. "A Multi-Species Synthesis of Physiological Mechanisms in Drought-
657 Induced Tree Mortality." *Nature Ecology and Evolution* 1(9):1285–91.

- 658 Akaike, Hirotugu. 1987. "Factor Analysis and AIC." Pp. 371–86 in. Springer, New York, NY.
- 659 Allen, Craig D. et al. 2010. "A Global Overview of Drought and Heat-Induced Tree Mortality Reveals
660 Emerging Climate Change Risks for Forests." *Forest Ecology and Management* 259(4):660–84.
- 661 Anderegg, W. R. L. et al. 2012. "From the Cover: The Roles of Hydraulic and Carbon Stress in a
662 Widespread Climate-Induced Forest Die-Off." *Proceedings of the National Academy of
663 Sciences* 109(1):233–37.
- 664 Anderegg, William R. L. 2015a. "Spatial and Temporal Variation in Plant Hydraulic Traits and Their
665 Relevance for Climate Change Impacts on Vegetation." *New Phytologist* 205(3):1008–14.
- 666 Anderegg, William R. L. et al. 2015b. "Tree Mortality from Drought, Insects, and Their Interactions in
667 a Changing Climate." *New Phytologist* 208(3):674–83.
- 668 Archambeau, Juliette et al. 2019. "Similar Patterns of Background Mortality across Europe Are
669 Mostly Driven by Drought in European Beech and a Combination of Drought and Competition
670 in Scots Pine." *Agricultural and Forest Meteorology*, 2020, vol. 280, p. 107772.
- 671 Arnold, Todd W. 2010. "Uninformative Parameters and Model Selection Using Akaike's Information
672 Criterion." *Journal of Wildlife Management* 74(6):1175–78.
- 673 Augspurger, Carol K. 2009. "Spring 2007 Warmth and Frost: Phenology, Damage and Refoliation in a
674 Temperate Deciduous Forest." *Functional Ecology* 23(6):1031–39.
- 675 Ball, J. Timothy, Ian E. Woodrow, and Joseph A. Berry. 1987. "A Model Predicting Stomatal
676 Conductance and Its Contribution to the Control of Photosynthesis under Different
677 Environmental Conditions." Pp. 221–24 in *Progress in photosynthesis research*. Springer.
- 678 Barnier, Julien, François Briatte, and Joseph Larmarange. 2018. "Question: Functions to Make
679 Surveys Processing Easier."
- 680 Bauch, Josef. 1986. "Characteristics and Response of Wood in Declining Trees from Forests Affected
681 by Pollution." *IAWA Journal* 7(4):269–76.
- 682 Beguería, Santiago and Sergio M. Vicente-Serrano. 2017. "SPEI: Calculation of the Standardised
683 Precipitation-Evapotranspiration Index."
- 684 Benito Garzón, Marta et al. 2018. "The Legacy of Water Deficit on Populations Having Experienced
685 Negative Hydraulic Safety Margin." *Global Ecology and Biogeography* 27(3):346–56.
- 686 Bigler, Christof and Harald Bugmann. 2018. "Climate-Induced Shifts in Leaf Unfolding and Frost Risk
687 of European Trees and Shrubs." *Scientific Reports* 8(1):1–10.
- 688 Brando, Paulo Monteiro et al. 2014. "Abrupt Increases in Amazonian Tree Mortality Due to Drought-
689 Fire Interactions." *Proceedings of the National Academy of Sciences of the United States of
690 America* 111(17):6347–52.
- 691 Bréda, Nathalie, Roland Huc, André Granier, and Erwin Dreyer. 2006. "Temperate Forest Trees and
692 Stands under Severe Drought : A Review of Ecophysiological Responses , Adaptation Processes
693 and Long-Term Consequences." *Annals of Forest Science* 63(6):625–44.
- 694 Brier, Glenn W. 1950. "Verification of Forecasts Expressed in Terms of Probability." *Monthly
695 Weather Review* 78(1):1–3.
- 696 De Caceres, Miquel, Nicolas Martin-StPaul, Marco Turco, Antoine Cabon, and Victor Granda. 2018.
697 "Estimating Daily Meteorological Data and Downscaling Climate Models over Landscapes."
698 *Environmental Modelling and Software* 186–96.
- 699 Cailleret, Maxime et al. 2017. "A Synthesis of Radial Growth Patterns Preceding Tree Mortality."
700 *Global Change Biology* 23(4):1675–90.
- 701 Cailleret, Maxime and Hendrik Davi. 2011. "Effects of Climate on Diameter Growth of Co-Occurring
702 *Fagus Sylvatica* and *Abies Alba* along an Altitudinal Gradient." *Trees* 25(2):265–76.
- 703 Campbell, Gaylon S. 1974. "A Simple Method for Determining Unsaturated Conductivity from
704 Moisture Retention Data." *Soil Science* 117(6):311–14.

- 705 Carnicer, Jofre et al. 2011. "Widespread Crown Condition Decline, Food Web Disruption, and
706 Amplified Tree Mortality with Increased Climate Change-Type Drought." *Proceedings of the*
707 *National Academy of Sciences* 108(4):1474–78.
- 708 Cavin, Liam and Alistair S. Jump. 2017. "Highest Drought Sensitivity and Lowest Resistance to
709 Growth Suppression Are Found in the Range Core of the Tree *Fagus Sylvatica* L. Not the
710 Equatorial Range Edge." *Global Change Biology* 23(1):362–79.
- 711 Cheaib, Alissar et al. 2012. "Climate Change Impacts on Tree Ranges: Model Intercomparison
712 Facilitates Understanding and Quantification of Uncertainty." *Ecology Letters* 15(6):533–44.
- 713 Choat, Brendan et al. 2018. "Triggers of Tree Mortality under Drought." *Nature* 558(7711):531–39.
- 714 Chuine, Isabelle, P. Cour, and D. D. Rousseau. 1999. "Selecting Models to Predict the Timing of
715 Flowering of Temperate Trees: Implications for Tree Phenology Modelling." *Plant, Cell and*
716 *Environment* 22(1):1–13.
- 717 Clark, James S. et al. 2011. "Individual-Scale Variation, Species-Scale Differences: Inference Needed
718 to Understand Diversity." *Ecology Letters* 14(12):1273–87.
- 719 Collet, Catherine and Gilles Le Moguedec. 2007. "Individual Seedling Mortality as a Function of Size,
720 Growth and Competition in Naturally Regenerated Beech Seedlings." *Forestry* 80(4):359–70.
- 721 Cowan, I. R. and G. D. Farquhar. 1977. "Stomatal Function in Relation to Leaf Metabolism and
722 Environment." *Symposia of the Society for Experimental Biology* 31:471–505.
- 723 Cribari-Neto, Francisco and Achim Zeileis. 2010. "Beta Regression in R." *Journal of Statistical*
724 *Software* 34(2).
- 725 Davi, H. et al. 2005. "Modelling Carbon and Water Cycles in a Beech Forest. Part II.: Validation of the
726 Main Processes from Organ to Stand Scale." *Ecological Modelling* 185(2–4):387–405.
- 727 Davi, H., C. Barbaroux, C. Francois, and E. Dufrêne. 2009. "The Fundamental Role of Reserves and
728 Hydraulic Constraints in Predicting LAI and Carbon Allocation in Forests." *Agricultural and*
729 *Forest Meteorology* 149(2):349–61.
- 730 Davi, Hendrik and Maxime Cailleret. 2017. "Assessing Drought-Driven Mortality Trees with
731 Physiological Process-Based Models." *Agricultural and Forest Meteorology* 232:279–90.
- 732 Dittmar, Christoph, Wolfgang Zech, and Wolfram Elling. 2003. "Growth Variations of Common
733 Beech (*Fagus Sylvatica* L.) under Different Climatic and Environmental Conditions in Europe—a
734 Dendroecological Study." *Forest Ecology and Management* 173(1–3):63–78.
- 735 Dobbertin, Matthias and Peter Brang. 2001. "Crown Defoliation Improves Tree Mortality Models."
736 *Forest Ecology and Management* 141(3):271–84.
- 737 Dufrêne et al. 2005. "Modelling Carbon and Water Cycles in a Beech Forest Part I : Model
738 Description and Uncertainty Analysis on Modelled NEE." *Ecological Modelling* 185:407–36.
- 739 Durand-Gillmann, Marion, Maxime Cailleret, Thomas Boivin, Louis Michel Nageleisen, and Hendrik
740 Davi. 2014. "Individual Vulnerability Factors of Silver Fir (*Abies Alba* Mill.) to Parasitism by Two
741 Contrasting Biotic Agents: Mistletoe (*Viscum Album* L. Ssp. *Abietis*) and Bark Beetles
742 (Coleoptera: Curculionidae: Scolytinae) during a Decline Process." *Annals of Forest Science*
743 71(6):659–73.
- 744 Farquhar, G. D., S. von Caemmerer, and J. A. Berry. 1980. "A Biochemical Model of Photosynthetic
745 CO₂ Assimilation in Leaves of C₃ Species." *Planta* 149(1):78–90.
- 746 Feng, Xue et al. 2018. "The Ecohydrological Context of Drought and Classification of Plant
747 Responses." *Ecology Letters*, November 1, 1723–36.
- 748 Gao, Shan et al. 2018. "Dynamic Responses of Tree-Ring Growth to Multiple Dimensions of
749 Drought." *Global Change Biology* 24(11):5380–90.
- 750 García-Plazaola, José Ignacio, Raquel Esteban, Koldobika Hormaetxe, Beatriz Fernández-Marín, and
751 José María Becerril. 2008. "Photoprotective Responses of Mediterranean and Atlantic Trees to
752 the Extreme Heat-Wave of Summer 2003 in Southwestern Europe." *Trees* 22(3):385–92.

- 753 Gausсен, H. 1958. "Le Hêtre Aux Pyrénées Espagnoles." Pp. 185–91 in Actas del tercer congreso
754 internacional de estudios pirenaicos, Gerona.
- 755 Gauzere, J. et al. 2017. "Integrating Interactive Effects of Chilling and Photoperiod in Phenological
756 Process-Based Models. A Case Study with Two European Tree Species: *Fagus Sylvatica* and
757 *Quercus Petraea*." *Agricultural and Forest Meteorology* 244–245:9–20.
- 758 Gillner, Sten, Nadja Ruger, Andreas Roloff, and Uta Berger. 2013. "Low Relative Growth Rates
759 Predict Future Mortality of Common Beech (*Fagus Sylvatica* L.)." *Forest Ecology and*
760 *Management* 302:372–78.
- 761 Granier, A., P. Biron, and D. Lemoine. 2000. "Water Balance, Transpiration and Canopy Conductance
762 in Two Beech Stands." *Agricultural and Forest Meteorology* 100(4):291–308.
- 763 Greenwood, Sarah et al. 2017. "Tree Mortality across Biomes Is Promoted by Drought Intensity,
764 Lower Wood Density and Higher Specific Leaf Area" edited by J. Chave. *ECOLOGY LETTERS*
765 20(4):539–53.
- 766 Hawkes, Corinna. 2000. "Woody Plant Mortality Algorithms: Description, Problems and Progress."
767 *Ecological Modelling* 126(2–3):225–48.
- 768 Hesse, Benjamin D., Michael Goisser, Henrik Hartmann, and Thorsten E. E. Grams. 2019. "Repeated
769 Summer Drought Delays Sugar Export from the Leaf and Impairs Phloem Transport in Mature
770 Beech" edited by M. Dannoura. *Tree Physiology* 39(2):192–200.
- 771 Hijmans, Robert J., Steven Phillips, John Leathwick, Jane Elith, and Maintainer Robert J. Hijmans.
772 2017. "Package 'Dismo.'" *Circles* 9(1):1–68.
- 773 Hosmer, David W. and Stanley Lemeshow. 2000. *Applied Logistic Regression*.
- 774 Hulsmann, Lisa et al. 2016. "Does One Model Fit All? Patterns of Beech Mortality in Natural Forests
775 of Three European Regions." *Ecological Applications* 26(8):2463–77.
- 776 Hulsmann, Lisa, Harald Bugmann, and Peter Brang. 2017. "How to Predict Tree Death from
777 Inventory Data – Lessons from a Systematic Assessment of European Tree Mortality Models -
778 SUPP." *Canadian Journal of Forest Research* (April):cjfr-2016-0224.
- 779 Hulsmann, Lisa, Harald Bugmann, Maxime Cailleret, and Peter Brang. 2018. "How to Kill a Tree:
780 Empirical Mortality Models for 18 Species and Their Performance in a Dynamic Forest Model."
781 *Ecological Applications* 28(2):522–40.
- 782 IGN. 2016. *La Mortalite*. France. https://inventaire-forestier.ign.fr/IMG/pdf/2018_mortalite.pdf
- 783 Jump, Alistair S., Jenny M. Hunt, and Josep Peñuelas. 2006. "Rapid Climate Change-Related Growth
784 Decline at the Southern Range Edge of *Fagus Sylvatica*." *Global Change Biology* 12(11):2163–
785 74.
- 786 Kneeshaw, Daniel D., Richard K. Kobe, K. David Coates, and Christian Messier. 2006. "Sapling Size
787 Influences Shade Tolerance Ranking among Southern Boreal Tree Species." *Journal of Ecology*
788 94(2):471–80.
- 789 Knutzen, Florian, Choimaa Dulamsuren, Ina Christin Meier, and Christoph Leuschner. 2017. "Recent
790 Climate Warming-Related Growth Decline Impairs European Beech in the Center of Its
791 Distribution Range." *Ecosystems* 20(8):1494–1511.
- 792 Kramer, Koen et al. 2010. "Modelling Exploration of the Future of European Beech (*Fagus Sylvatica*
793 L.) under Climate Change-Range, Abundance, Genetic Diversity and Adaptive Response."
794 *Forest Ecology and Management* 259(11):2213–22.
- 795 Lebourgeois, F., N. Breda, E. Ulrich, and A. Granier. 2005. "Climate-Tree-Growth Relationships of
796 European Beech (*Fagus Sylvatica* L.) in the French Permanent Plot Network (RENECOFOR)."
797 *Trees* 19:385–401.
- 798 Lenz, Armando, Gunter Hoch, Yann Vitasse, and Christian Korner. 2013. "European Deciduous Trees
799 Exhibit Similar Safety Margins against Damage by Spring Freeze Events along Elevational
800 Gradients." *New Phytologist* 200(4):1166–75.

- 801 Lines, Emily R., David A. Coomes, and Drew W. Purves. 2010. "Influences of Forest Structure,
802 Climate and Species Composition on Tree Mortality across the Eastern US" edited by A.
803 Hector. PLoS ONE 5(10):e13212.
- 804 Long, Jacob A. 2018. "Jtools: Analysis and Presentation of Social Scientific Data."
- 805 Lorenz, Martin and Georg Becher. 2012. Forest Condition in Europe.
- 806 Loustau, D., A. Granier, F. El Hadj Moussa, M. Sartore, and M. Guedon. 1990. "Evolution Saisonnière
807 Du Flux de Sève Dans Un Peuplement de Pins Maritimes." *Annales Des Sciences Forestières*
808 47(6):599–618.
- 809 Van Mantgem, Phillip J. et al. 2009. "Widespread Increase of Tree Mortality Rates in the Western
810 United States." *Science* 323(5913):521–24.
- 811 Maraun, Mark, Jörg-Alfred Salamon, Katja Schneider, Matthias Schaefer, and Stefan Scheu. 2003.
812 "Oribatid Mite and Collembolan Diversity, Density and Community Structure in a Moder
813 Beech Forest (*Fagus Sylvatica*): Effects of Mechanical Perturbations." *Soil Biology and*
814 *Biochemistry* 35(10):1387–94.
- 815 Martin, George L. and Alan R. Ek. 1984. "A Comparison of Competition Measures and Growth
816 Models for Predicting Plantation Red Pine Diameter and Height Growth." *Forest Science*
817 30(3):731–43.
- 818 McDowell, Nate G. et al. 2013. "Evaluating Theories of Drought-Induced Vegetation Mortality Using
819 a Multimodel-Experiment Framework." *New Phytologist* 200(2):304–21.
- 820 McDowell, Nate G. et al. 2011. "The Interdependence of Mechanisms Underlying Climate-Driven
821 Vegetation Mortality." *Trends in Ecology & Evolution* 26(10):523–32.
- 822 Meir, Patrick, Maurizio Mencuccini, and Roderick C. Dewar. 2015. "Drought-Related Tree Mortality:
823 Addressing the Gaps in Understanding and Prediction." *New Phytologist* 207(1):1443–47.
- 824 Menzel, Annette, Raimund Helm, and Christian Zang. 2015. "Patterns of Late Spring Frost Leaf
825 Damage and Recovery in a European Beech (*Fagus Sylvatica* L.) Stand in South-Eastern
826 Germany Based on Repeated Digital Photographs." *Frontiers in Plant Science* 6:110.
- 827 Monserud, Robert A. 1976. "Simulation of Forest Tree Mortality." *Forest Science* 22(4):438–44.
- 828 Monteith, J. L. 1965. "Evaporation and Environment. The State and Movement of Water in Living
829 Organisms. Symposium of the Society of Experimental Biology, Vol. 19 (Pp. 205-234)."
- 830 Mueller, Rebecca C. et al. 2005. "Differential Tree Mortality in Response to Severe Drought:
831 Evidence for Long-Term Vegetation Shifts." *Journal of Ecology* 93(6):1085–93.
- 832 Niinemets, Ülo. 2010. "Responses of Forest Trees to Single and Multiple Environmental Stresses
833 from Seedlings to Mature Plants: Past Stress History, Stress Interactions, Tolerance and
834 Acclimation." *Forest Ecology and Management* 260(10):1623–39.
- 835 Nourtier, Marie et al. 2014. "Transpiration of Silver Fir (*Abies Alba* Mill.) during and after Drought in
836 Relation to Soil Properties in a Mediterranean Mountain Area." *Annals of Forest Science*
837 71(6):683–95.
- 838 O'Brien, Michael J. et al. 2017. "A Synthesis of Tree Functional Traits Related to Drought-Induced
839 Mortality in Forests across Climatic Zones. *Journal of Applied Ecology* 54(6):1669–86.
- 840 O'Brien, Michael J., Sebastian Leuzinger, Christopher D. Philipson, John Tay, and Andy Hector. 2014.
841 "Drought Survival of Tropical Tree Seedlings Enhanced by Non-Structural Carbohydrate
842 Levels." *Nature Climate Change* 4(8):710–14.
- 843 Pammenter NW and Vander Willigen C. 1998. "A Mathematical and Statistical Analysis of the Curves
844 Illustrating Vulnerability of Xylem to Cavitation." *Tree Physiology* 18(Equation 1):589–593.
- 845 Penuelas, Josep and Martí Boada. 2003. "A Global Change-Induced Biome Shift in the Montseny
846 Mountains (NE Spain)." *Global Change Biology* 9(2):131–40.
- 847 Perci du Sert, Th. 1982. Relations Entre La Phenologie et La Morphologie Du Hêtre Dans Le Massif
848 Des Albères.

- 849 Pretzsch, Hans. 1996. "Growth Trends of Forests in Southern Germany." Pp. 107–31 in Growth
850 Trends in European Forests. Berlin, Heidelberg: Springer Berlin Heidelberg.
- 851 Robson, T. Matthew, Erwin Rasztovits, Pedro J. Aphalo, Ricardo Alia, and Ismael Aranda. 2013.
852 "Flushing Phenology and Fitness of European Beech (*Fagus Sylvatica* L.) Provenances from a
853 Trial in La Rioja, Spain, Segregate According to Their Climate of Origin." *Agricultural and Forest
854 Meteorology* 180:76–85.
- 855 Ryan, Michael G. 1991. "Effects of Climate Change on Plant Respiration." *Ecological Applications*
856 1(2):157–67.
- 857 Sala, A. and J. D. Tenhunen. 1996. "Simulations of Canopy Net Photosynthesis and Transpiration in
858 *Quercus Ilex* L. under the Influence of Seasonal Drought." *Agricultural and Forest Meteorology*
859 78(3–4):203–22.
- 860 Schielzeth, Holger. 2010. "Simple Means to Improve the Interpretability of Regression Coefficients."
861 *Methods in Ecology and Evolution* 1(2):103–13.
- 862 Seidl, Rupert et al. 2011. "Modelling Natural Disturbances in Forest Ecosystems: A Review."
863 *Ecological Modelling* 222(4):903–24.
- 864 Senf, Cornelius et al. 2018. "Canopy Mortality Has Doubled in Europe's Temperate Forests over the
865 Last Three Decades." *Nature Communications* 9(1):4978.
- 866 Sevanto, Sanna, Nate G. McDowell, L. Turin Dickman, Robert Pangle, and William T. Pockman. 2014.
867 "How Do Trees Die? A Test of the Hydraulic Failure and Carbon Starvation Hypotheses." *Plant,
868 Cell and Environment* 37(1):153–61.
- 869 Stadt, Kenneth J. et al. 2007. "Evaluation of Competition and Light Estimation Indices for Predicting
870 Diameter Growth in Mature Boreal Mixed Forests." *Annals of Forest Science* 64(64):477–90.
- 871 Thuiller, Wilfried, Sandra Lavorel, M. B. Araujo, Martin T. Sykes, and I. Colin Prentice. 2005. "Climate
872 Change Threats to Plant Diversity in Europe." *Proceedings of the National Academy of
873 Sciences* 102(23):8245–50.
- 874 Tyree, M. T. and J. S. Sperry. 1989. "Vulnerability of Xylem to Cavitation and Embolism." *Annual
875 Review of Plant Physiology and Plant Molecular Biology* 40(1):19–36.
- 876 Vanoni, Marco, Harald Bugmann, Magdalena Nötzli, and Christof Bigler. 2016. "Drought and Frost
877 Contribute to Abrupt Growth Decreases before Tree Mortality in Nine Temperate Tree
878 Species." *Forest Ecology and Management Journal* 382:51–63.
- 879 Vidal, Jean-Philippe, Eric Martin, Laurent Franchistéguy, Martine Baillon, and Jean-Michel
880 Soubeyroux. 2010. "A 50-Year High-Resolution Atmospheric Reanalysis over France with the
881 Safran System." *International Journal of Climatology* 30(11):1627–44.
- 882 Vitasse, Yann et al. 2009. "Leaf Phenology Sensitivity to Temperature in European Trees: Do within-
883 Species Populations Exhibit Similar Responses?" *Agricultural and Forest Meteorology*
884 149(5):735–44.
- 885 De Vries, F. W. T. Pennin., A. H. M. Brunsting, and H. H. Van Laar. 1974. "Products, Requirements
886 and Efficiency of Biosynthesis a Quantitative Approach." *Journal of Theoretical Biology*
887 45(2):339–77.

888

889 Appendices

890 Four supplementary appendices are available on bioRxiv (XXX):

891 Appendix 1: Beta-regression model for mortality rate at population-level

892 Appendix 2: CASTANEA calibration and simulations

893 Appendix 3: Logistic regression models for the probability of mortality at tree-level

894 Appendix 4: survival analysis the probability of mortality at tree- and year-levels